Electronic Supplementary Material (ESI) for Environmental Science: Nano.
This journal is © The Royal Society of Chemistry 2022

Supplemental information for

Metals binding processes on Nanoplastics :

Rare earth elements as a probe

Florent Blancho[1], Mélanie Davranche[1], Rémi Marsac[1], Adrien Léon[1], Aline Dia[1], Bruno Grassl[2], Stéphanie[2] Reynaud, and Julien Gigault[1,3],*

[1]Laboratoire Géosciences Rennes, UMR6118, 263 Avenue Général Leclerc, 35042 Rennes

[2.] IPREM, CNRS / Université de Pau et des Pays de L'Adour, F64000 Pau, France

[3] TAKUVIK laboratoy, UMI3376 CNRS/Université Laval, Québec, Canada

E-mail contact: julien gigault@takuvik.ulaval.ca

S1. NPs characterization

The hydrodynamic radius, Hr, of the NPs was determined using Dynamic Light Scattering (DLS) (VASCO Flex's, Cordouan Technologies) for suspensions concentrated at 10 ppm without Ionic Strength (IS) (Figure S1). For PSLs, DLS indicated, as expected, a monodisperse suspension (i.e. straight Log-transformed ACF) (Figure S2). As a result, no uncontrolled aggregation occurred. Their Hr were considered as equal to 200 nm for the $PSL_{surfactant}$ (NIST CMRs) and 380 nm for the PSL_{free} (1).

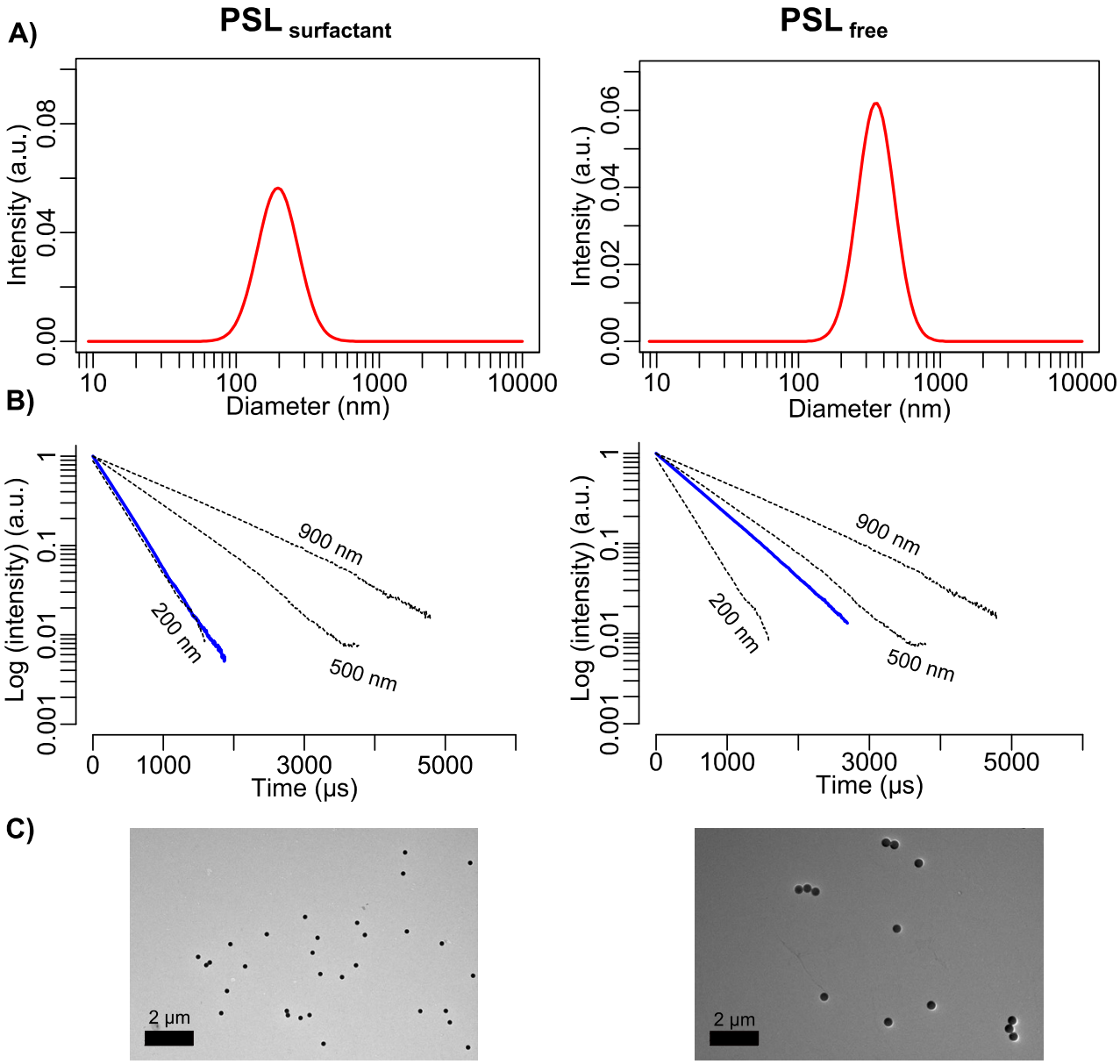

Figure S1. Size characterisation of PSL model. A) Population size from SBL modelling. B) Log-transformed time-ACF of the intensity of light scattered compare to CMRs standards. C) TEM pictures from the suspensions.

For e-NPs, Both log-transformed slopes of the autocorrelation function (ACF) were inferior to the 900 nm of the CMRs standard (Blue line, 2A), indicating that Hr was inferior to 900 nm. Moreover, their log-transformed ACF were not straight compared to the CMRs indicating polymodal

suspensions. This result is coherent with the bimodal distribution proposed by the Sparse Bayesian Learning, SBL, based-modelling of the ACF (2B), the first and second population size have an average Hr of 226 ± 36 and 376 ± 64 nm.

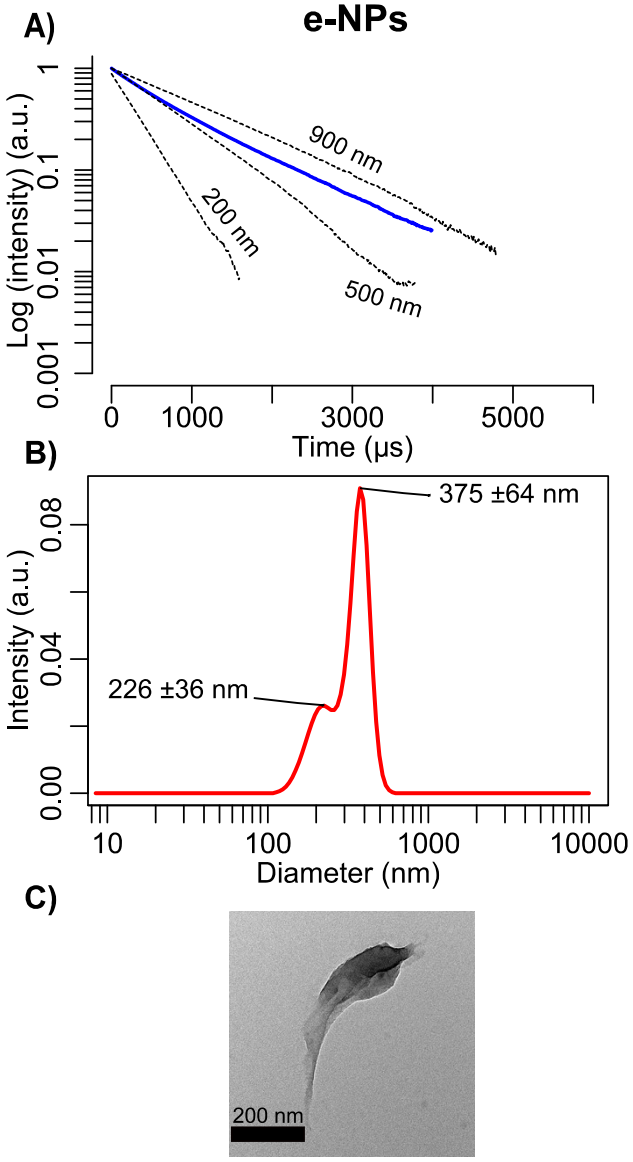

Figure S2. Size characterisation the e-NPs model. A) Log-transformed time-ACF of the intensity of light scattered compare to CMRs standards. B) Population size from SBL modelling. C) TEM pictures from the suspensions.

The geometric shape of NPs was observed by transmission electronic microscopy (TEM) (JEM 2100 HR, Jeol). Transmission electronic microscopy was operated at 200-kV acceleration voltage with a LaB_6 as electron source, the point and line resolution are of 2.3 Å and 1.4 Å, respectively. Particles were photographed with a Gatan Orius SC200D camera, and elemental analysis was performed using an EDX Oxford X-Max 80T detector. The TEM observations showed anisotropic NPs (Figure S1C and S2C), as previously observed by (2).

The specific surface area (SSA) of NPs was determined by the BET method (Brunnauer Emmet and Teller) for e-NPs while it was extrapolated from the particle diameter for PSLs (Table S1). The BET

analyses were carried out using with a Gemini VII instrument (Micromeritics) for e-NPs and m-NPs while extrapolated from the particle diameter for the spherical PSL. The determined SSA are reported in the Table S1.

The surface ionizable group was assessed by potentiometric titration using a Titrano unit controlled by the Tiamo software (Metrohm). All solutions were titrated with 0.01 M NaOH (Honeywell Fluka), under a N_2 flux. Prior titration, the pH probe was calibrated on a concentration scale using 1mM HNO_3. Titration were performed at 10, 100 and 1000 mM of $NaNO_3$ as IS and started below pH 4 by adding a fixed volume of 100mM HNO_3. The determination of the protonable groups was performed as describe by Spadini et al, 2018 (3). Briefly, the proton released from the surface, H_{surf}, was related to the pH of the solution (Eq. S1). The total surface site concentration $Hs_{tot,}$ was defined as the released H_{surf} between pH 4 and 8.0 for the highest IS. The CO_2 diffusion during the titration was taken in account using the Hs_{tot} of the ultrapure water (Blank).

$$[H^+] = [H_{init}] + [H_{base}] + [H_{surf}] + [OH^-] \qquad \text{(S1)}$$

With, $[H^+]$, the free proton concentration, (M), $[H_{init}]$, the concentration of acid added to fix the pH below pH 4 (M), $[H_{base}]$, the concentration of base added during the titration (M), positive when base is used and negative when acid is used, $[H_{surf}]$, the concentration of the released H^+, the only unknown (M) and $[OH^-]$, the concentration of the H^+ released from the water auto-protolyze, at pH 7 (M).

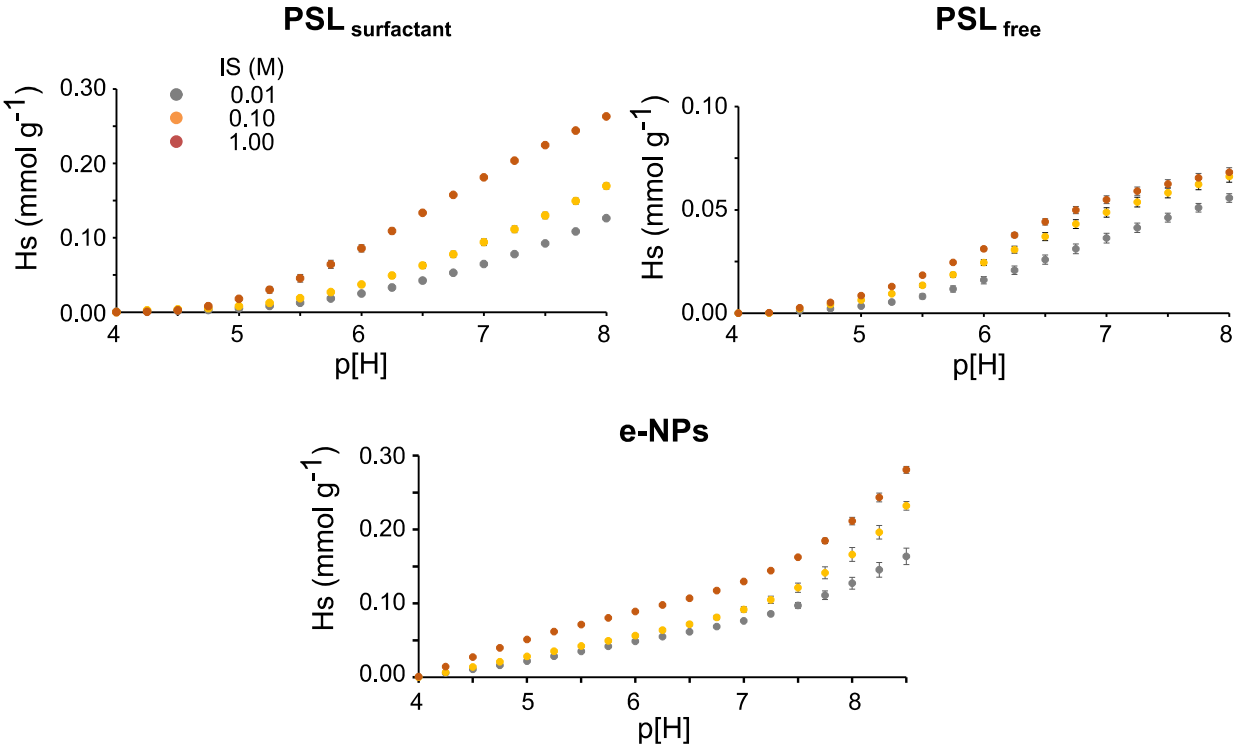

Figure S3. Evolution of the Hs with the pH for both PSLs and e-NPs at 3 IS: 0.01, 0.10, 1.00 M.

As expected, the dissociation of the surface group increased with the increasing pH (Eq. 3). The IS promoted the deprotonation of surface group by decreasing the diffuse layer length and thus shielding the electrostatic impact of Ψ_0 (4). For both PSLs, titrations at 1M IS showed a typical sigmoidal curve (5,6) (Figure S3). These titration curve indicates that the whole ionizable group was dissociated between pH 4 and 8. The total surface ionizable group, Hs_{tot}, was considered to be equal to the concentration of the deprotonated group at pH 8, as a plateau was reached for both PSLs. The Hs_{tot} was determined as $0.263 \pm 2\ 10^{-3}$ and $0.068 \pm 2\ 10^{-3}$ mmol g^{-1} for the $PSL_{surfactant}$ and PSL_{free}, respectively. According to the SSA, the site density was 5.65 and 2.78 sites nm^{-2} for $PSL_{surfactant}$ and PSL_{free}, respectively. The Hs_{tot} and site density are higher for $PSL_{surfactant}$.

For e-NPs, the 1M titration curves were not sigmoidal and showed the same increase after pH 7.5 (Figure S3) avoiding the Hs_{tot} determination (no plateau was reached). However, the total concentration of surface site could be estimated (value obtained for the highest pH, ≈ 8.5) as $\geq 0.281 \pm 5\ 10^{-3}$. According to the SSA, the site density was ≥ 14.22 sites nm^{-2}. The Hs_{tot} and site density are higher for $PSL_{surfactant}$.

Table S1. Specific surface area, surface ionizable group and site density of the studied NPs.

NPs	SSA ($m^2\ g^{-1}$ C)	Hs_{tot} (mmol g^{-1} C)	Site density (Sites nm^{-2})
$PSL_{surfactant}$	30.49	0.281	5.65
PSL_{free}	16.00	0.068	2.78
e-NPs	13.90	0.281	≥14.22

S2. La/Lu and La/Sm ratios evolution for each NPs

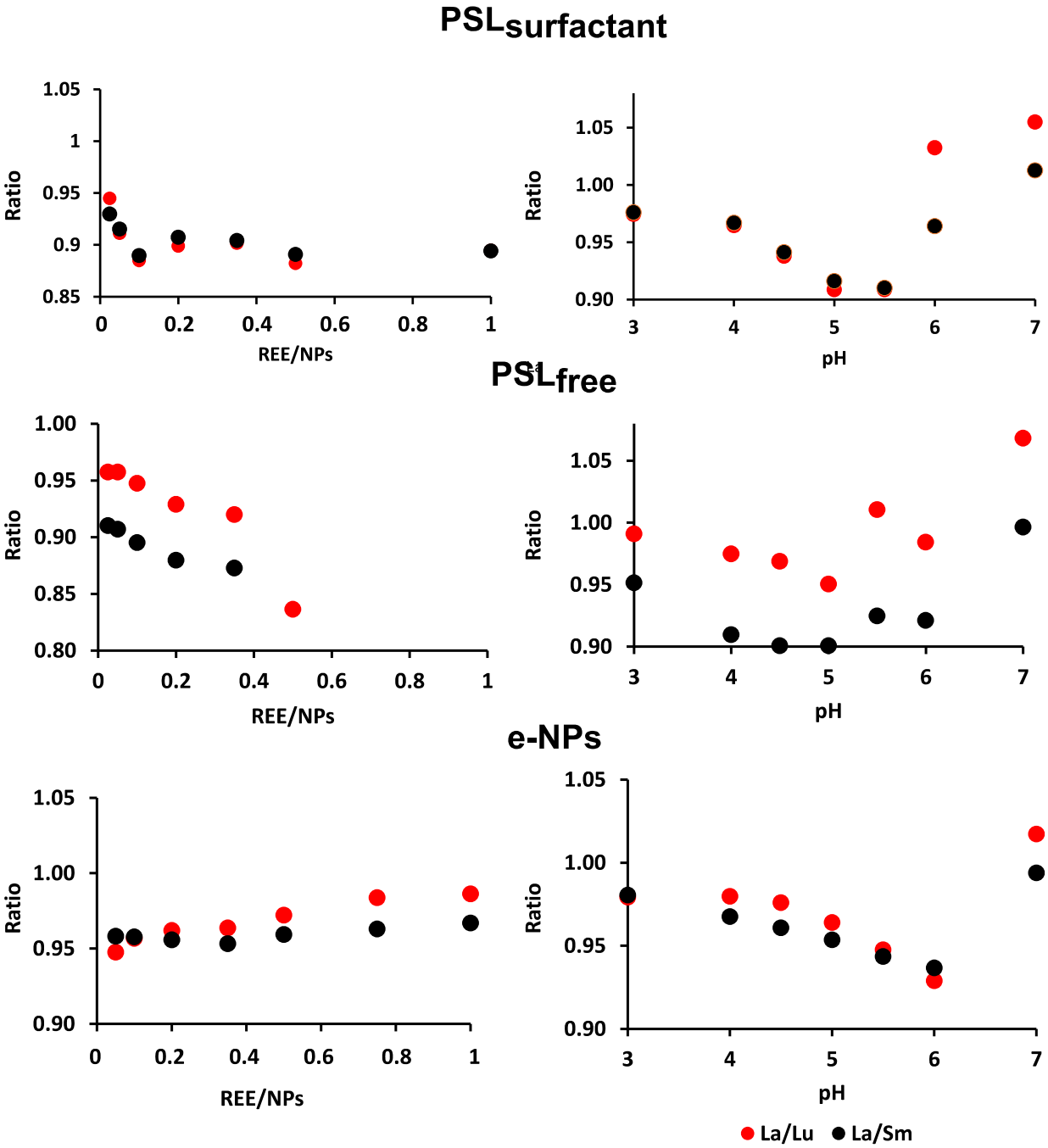

Figure S4. Evolution of the La/Lu and La/Sm of the REE pattern obtained relative to the REE/NPs ratio and pH for both PSLs and e-NPs.

S3. Log K_{REE} references

Table 2. Organic ligand REE stability constant references used in Figure 4.

Acid	Metal complex	IS (M)	Temp. (°C)	References
Acetate	1:1	0.1	25	(7)
	1:2	0.1		
	1:3	1		
Propionate	1:1	1		
	1:2	0.1		
Isobutyrate	1:1	1		
Diethylmalonate	1:1	0.1		
DL-2-Hydroxybutanoate	1:1	0.1		
Lactate	1:1	0.1		
Oxalate	1:1	0		(8)

References

1. Pessoni L, Veclin C, El Hadri H, Cugnet C, Davranche M, Pierson-Wickmann A-C, et al. Soap- and metal-free polystyrene latex particles as a nanoplastic model. Environ Sci: Nano. 2019;6(7):2253-8.

2. Blancho F, Davranche M, Fumagalli F, Ceccone G, Gigault J. A reliable procedure to obtain environmentally relevant nanoplastic proxies. ES nano. 2021;

3. Spadini L, Navel A, Martins JMF, Vince E, Lamy I. Soil aggregates: a scale to investigate the densities of metal and proton reactive sites of organic matter and clay phases in soil. Eur J Soil Sci. sept 2018;69(5):953-61.

4. Pfeiffer C, Rehbock C, Hühn D, Carrillo-Carrion C, de Aberasturi DJ, Merk V, et al. Interaction of colloidal nanoparticles with their local environment: the (ionic) nanoenvironment around nanoparticles is different from bulk and determines the physico-chemical properties of the nanoparticles. J R Soc Interface. 6 juill 2014;11(96):20130931.

5. Connors KA. Chemical kinetics: the study of reaction rates in solution. New York, N.Y: VCH; 1990. 480 p.

6. Chen J, Hu J, Xu Y, Krasny R, Geng W. Computing Protein pKas Using the TABI Poisson–Boltzmann Solver. J Comput Biophys Chem. mars 2021;20(02):175-87.

7. Martell AE, Smith RM. Other Organic Ligands [Internet]. Boston, MA: Springer US; 1977 [cité 23 févr 2021]. Disponible sur: http://link.springer.com/10.1007/978-1-4757-1568-2

8. Wood SA. The aqueous geochemistry of the rare-earth elements: Critical stability constants for complexes with simple car□ylic acids at 25°C and 1 bar and their application to nuclear waste management. Engineering Geology. sept 1993;34(3-4):229-59.